Vemurafenib Redifferentiation of *BRAF* Mutant, RAI-Refractory Thyroid Cancers

Lara A. Dunn,[1,2] Eric J. Sherman,[1,2] Shrujal S. Baxi,[1,2] Vatche Tchekmedyian,[1] Ravinder K. Grewal,[3] Steven M. Larson,[3] Keith S. Pentlow,[4] Sofia Haque,[3] R. Michael Tuttle,[1] Mona M. Sabra,[1] Stephanie Fish,[1] Laura Boucai,[1] Jamie Walters,[1] Ronald A. Ghossein,[5] Venkatraman E. Seshan,[6] Ai Ni,[6] Duan Li,[7] Jeffrey A. Knauf,[8] David G. Pfister,[1,2] James A. Fagin,[1,2,8] and Alan L. Ho[1,2]

[1]Department of Medicine, Memorial Sloan-Kettering Cancer Center, New York, New York 10065; [2]Department of Medicine, Weill Cornell Medical College, New York, New York 10065; [3]Department of Radiology, Memorial Sloan-Kettering Cancer Center, New York, New York 10065; [4]Department of Medical Physics, Memorial Sloan-Kettering Cancer Center, New York, New York 10065; [5]Department of Pathology, Memorial Sloan-Kettering Cancer Center, New York, New York 10065; [6]Department of Epidemiology–Biostatistics, Memorial Sloan-Kettering Cancer Center, New York, New York 10065; [7]Department of Radiology, Memorial Sloan-Kettering Cancer Center, New York, New York 10065; and [8]Human Oncology and Pathogenesis, Memorial Sloan-Kettering Cancer Center, New York, New York 10065

ORCiD numbers: 0000-0002-6885-3742 (A. L. Ho).

Context: *BRAF*^{V600E} mutant thyroid cancers are often refractory to radioiodine (RAI).

Objectives: To investigate the utility and molecular underpinnings of enhancing lesional iodide uptake with the BRAF inhibitor vemurafenib in patients with RAI-refractory (RAIR).

Design: This was a pilot trial that enrolled from June 2014 to January 2016.

Setting: Academic cancer center.

Patients: Patients with RAIR, *BRAF* mutant thyroid cancer.

Intervention: Patients underwent thyrotropin-stimulated iodine-124 (^{124}I) positron emission tomography scans before and after ~4 weeks of vemurafenib. Those with increased RAI concentration exceeding a predefined lesional dosimetry threshold (^{124}I responders) were treated with iodine-131 (^{131}I). Response was evaluated with imaging and serum thyroglobulin. Three patients underwent research biopsies to evaluate the impact of vemurafenib on mitogen-activated protein kinase (MAPK) signaling and thyroid differentiation.

Main Outcome Measure: The proportion of patients in whom vemurafenib increased RAI incorporation to warrant ^{131}I.

Results: Twelve *BRAF* mutant patients were enrolled; 10 were evaluable. Four patients were ^{124}I responders on vemurafenib and treated with ^{131}I, resulting in tumor regressions at 6 months. Analysis of research tumor biopsies demonstrated that vemurafenib inhibition of the MAPK pathway was associated with increased thyroid gene expression and RAI uptake. The mean pretreatment serum thyroglobulin value was higher among ^{124}I responders than among nonresponders (30.6 vs 1.0 ng/mL; $P = 0.0048$).

ISSN Print 0021-972X ISSN Online 1945-7197
Printed in USA

Received 6 July 2018. Accepted 20 September 2018.
First Published Online 25 September 2018

Abbreviations: BRS, BRAF/RAS score; eTDS, enhanced thyroid differentiation score; FDG, ^{18}F-fluorodeoxyglucose; MAPK, mitogen-activated protein kinase; MTA, maximum tolerable activity; NIS, Na^+/I^- symporter; PET, positron emission tomography; PR, partial response; PTC, papillary thyroid carcinoma; RAI, radioiodine; RAIR, radioiodine refractory; RECIST, Response Evaluation Criteria in Solid Tumors; RNAseq, RNA sequencing; SD, stable disease; SUV_{max}, maximum standardized uptake value; TCGA, The Cancer Genome Atlas; TDS, thyroid differentiation score; TG, thyroglobulin; TKI, tyrosine kinase inhibitor; TPO, thyroid peroxidase.

Conclusions: Vemurafenib restores RAI uptake and efficacy in a subset of *BRAF* mutant RAIR patients, probably by upregulating thyroid-specific gene expression via MAPK pathway inhibition. Higher baseline thyroglobulin values among responders suggest that tumor differentiation status may be a predictor of vemurafenib benefit. (***J Clin Endocrinol Metab*** **104: 1417–1428, 2019)**

Radioiodine-refractory (RAIR) thyroid cancers lose the ability to efficiently concentrate iodide, rendering RAI [iodine-131 (^{131}I] ineffective. Although the tyrosine kinase inhibitors (TKIs) sorafenib and lenvatinib are standard treatments for patients with RAIR thyroid cancer (1–4), a limitation of these therapies is the need for continuous dosing and the accompanying drug toxicities (1, 4, 5).

A strategy to restore the capacity of RAIR tumors to trap and respond to a single administration of ^{131}I (redifferentiation) without maintenance drug therapy could replace or defer the need for TKIs. Approximately 70% of papillary thyroid cancers possess mutually exclusive oncogenic mutations of genes encoding effectors of the mitogen-activated protein kinase (MAPK) pathway (6), the most common of which is $BRAF^{V600E}$ (~60%) (7). Constitutive MAPK pathway activation promotes RAI refractoriness by suppressing the expression of genes that mediate iodide uptake and thyroid hormone biosynthesis [*e.g.,* Na^+/I^- symporter (NIS), thyroid peroxidase (TPO), and thyroglobulin (TG)] (8–14). We previously demonstrated in genetically engineered mouse models of *BRAF* mutant thyroid cancer that MAPK pathway inhibition restores the expression of these genes to increase tumor RAI avidity (15, 16). We translated these findings into a clinical trial in which iodine-124 (^{124}I) positron emission tomography (PET) CT lesional dosimetry demonstrated that the MEK 1/2 allosteric inhibitor selumetinib (AstraZeneca) could restore RAI efficacy in a subset of RAIR patients (17). The degree of benefit observed depended on the mutation present; whereas all five *NRAS* mutant patients benefited, only one of nine *BRAF* mutant patients achieved sufficient RAI tumor incorporation to justify ^{131}I.

We hypothesized that improving outcomes in the *BRAF* mutant group would require more potent MAPK pathway inhibition. Vemurafenib is an ATP-competitive BRAF inhibitor that abrogates monomeric $BRAF^{V600E}$ signaling and paradoxically activates BRAF wild-type dimers in normal cells (18), resulting in a wide therapeutic window for robust MAPK inhibition in tumor cells. Notably, a pilot trial did report that a subset of *BRAF* mutant patients can develop new RAI enhancement in metastatic lesions with the BRAF inhibitor dabrafenib (Novartis) (19). We conducted a clinical trial to evaluate how effectively vemurafenib can mediate the clinical and molecular redifferentiation of *BRAF* mutant RAIR thyroid cancers. The insights from this trial not previously addressed in previous studies include the differential contribution of drug-induced regression vs increase in ^{131}I efficacy, quantitative measurements of RAI-enhanced incorporation with ^{124}I PET scans, investigation of the transcriptomic changes associated with BRAF inhibitor–mediated redifferentiation in serial research biopsies, and evidence that baseline TG level could be a predictor of benefit for this therapeutic approach.

Materials and Methods

Patient population

This was a single-center, 10-patient pilot study. The trial was approved by the Institutional Review Board at Memorial Sloan-Kettering Cancer Center. Subjects provided written informed consent. Eligible patients were required to have a thyroid carcinoma of follicular cell origin with a *BRAF* mutation at V600 detected in a Clinical Laboratory Improvement Amendments–certified or US Food and Drug Administration–approved assay. Patients with anaplastic and Hurthle cell cancers were excluded. One of the following criteria for RAI-refractory disease had to be met: a metastatic lesion lacking RAI avidity on a diagnostic scan performed ≤2 years before enrollment, an RAI-avid metastatic lesion that remained stable in size or progressed despite RAI therapy ≥6 months before study entry, or at least one ^{18}F-fluorodeoxyglucose (FDG)-avid lesion with a maximum standardized uptake value (SUV_{max}) ≥5 (given the inverse relationship between FDG and RAI avidity) (20). Patients were not allowed treatment with ^{131}I <6 months before study treatment or radiation, chemotherapy, or targeted therapy <4 weeks before. Two research biopsies were mandatory, except for patients with inaccessible tumors or those for whom a biopsy was deemed too risky (*e.g.,* a platelet count <100,000/μL).

Study design

Figure 1 illustrates the study schema. Baseline RAI avidity was assessed with ^{124}I PET/CT lesional dosimetry while patients were on a low-iodine diet (initiated 5 days before) (21). Patients were given 0.9 mg thyrotropin alfa (Thyrogen, Sanofi Genzyme) by intramuscular injection for 2 consecutive days, followed by 6 mCi (range: 4.8 to 7.2 mCi) of ^{124}I (IBA Molecular, later Zevacor and now Sofie Biosciences) on the third day. PET/CT scan images were obtained on day 5. Patients then initiated vemurafenib 960 mg orally twice daily for ~4 weeks. During the fourth week of therapy, the ^{124}I PET/CT lesional dosimetry was repeated. If at least one index tumor (≥5 mm in maximal diameter) was predicted to

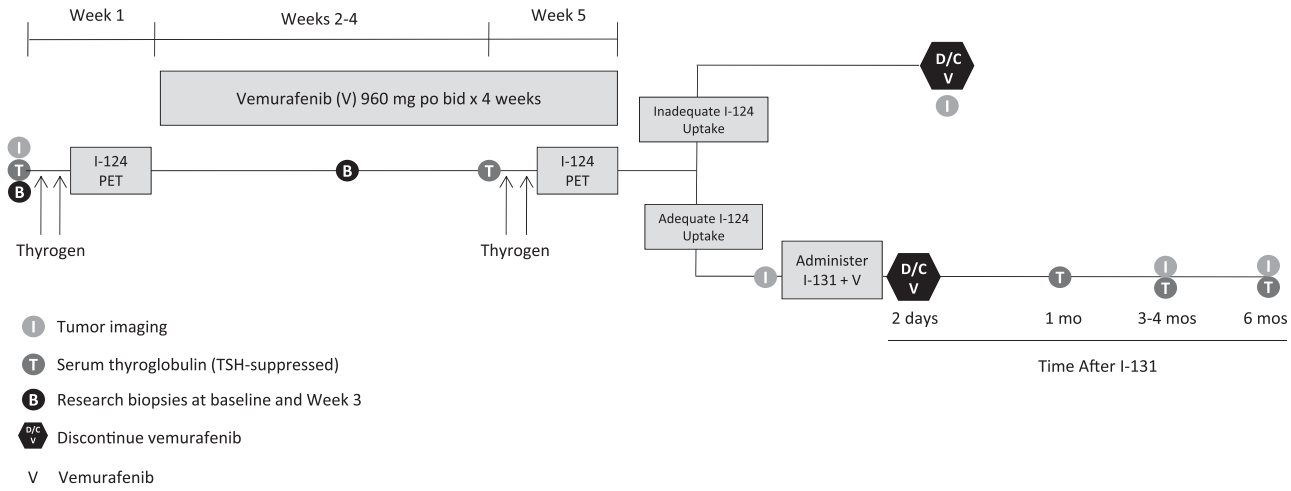

Figure 1. Study schema. After a baseline Thyrogen-stimulated ^{124}I PET scan, patients were treated with ~4 wk of vemurafenib (960 mg orally twice daily), and then re-evaluated with a second ^{124}I PET scan. If an index tumor met the lesional dosimetry criteria [≥2000 cGy achieved with ≤300 mCi of ^{131}I (^{124}I responder)], patients were continued on vemurafenib and treated with ^{131}I. Vemurafenib was discontinued (D/C) 2 d after ^{131}I. Efficacy was measured with imaging at baseline, after vemurafenib alone, and ~3 mo and 6 mo after ^{131}I. In three patients, two research biopsies were performed before treatment and then 10 to 11 d on vemurafenib.

absorb ≥2000 cGy with a clinically administered ^{131}I activity of ≤300 mCi, then the patient was categorized as an ^{124}I responder. These patients continued vemurafenib and underwent Thyrogen-stimulated whole-body and blood dosimetry to determine the maximum tolerable activity (MTA) (the predicted maximal ^{131}I activity that could be administered without bone marrow or pulmonary toxicity) (22–24). A therapeutic ^{131}I activity under or at the MTA was then administered with Thyrogen stimulation (25). Vemurafenib was discontinued 2 days after ^{131}I. Patients for whom the second ^{124}I PET/CT did not show sufficient iodide uptake were designated ^{124}I nonresponders and removed. Among ^{124}I responders, imaging was performed after ~4 weeks of vemurafenib alone, and then 3 and 6 months after ^{131}I.

For ^{124}I nonresponders, scans were performed within 1.5 months of vemurafenib discontinuation. Serum TG levels were measured before treatment, after vemurafenib, and 1, 3, and 6 months after ^{131}I. On 2 March 2015, the TG assay changed from the Brahms GmBH (ThermoFisher; used for patients 1 to 6) to the chemiluminescent assay on the Beckman Access (used for patients 6 to 12). The Brahms GmBH assay is a recovery assay that was developed before the international standardization of TG. The standard used was half the value of the international standard. Therefore, all TG values obtained on the Beckman Access assay that uses the international standard are reported here at one-half the calculated value to make them comparable to those obtained with the Brahms GmBH assay.

Molecular studies

Biopsies were performed before and during treatment (10 to 11 days of vemurafenib) on the same tumor in three patients for RNA sequencing (RNAseq). For RNA extraction, frozen tissue was homogenized in Trizol and RNA was extracted with chloroform. Isopropanol and linear acrylamide were added, and the RNA was precipitated with 75% ethanol. Samples were resuspended in RNase-free water. After RiboGreen quantification and quality control by Agilent BioAnalyzer, 0.59-1μg of total RNA with an RNA integrity number varying from 7.1 to 8.6 underwent ribosomal depletion and library preparation using the TruSeq Stranded Total RNA LT Kit (Illumina catalog # RS-122-1202) according to instructions provided by the manufacturer with 6 cycles of PCR. Samples were barcoded and run on a HiSeq 2500 in a 50 bp/50 bp paired end run, using the TruSeq SBS Kit v4 (Illumina). On average, 89 million paired reads were generated per sample and 25% of the data mapped to the transcriptome. Reads were aligned [Spliced Transcripts Alignment to a Reference (STAR)] and normalized (reads per kilobase per million) with Partek® Flow (Partek). The MAPK output gene set contained the 52 genes described by Pratilas *et al.* (26) and used by The Cancer Genome Atlas (TCGA) (7) to measure the transcriptional output of the MAPK pathway (Table 1). The BRAF/RAS score (BRS) gene set contained the 71 genes identified by TCGA (7) to distinguish $BRAF^{V600E}$ papillary thyroid carcinomas (PTCs) from those expressing oncogenic RAS mutations (Table 1). The thyroid differentiation score (TDS) gene list consisted of the 16 genes used by the TCGA (7) (Table 1). The enhanced thyroid differentiation score (eTDS) positive [eTDS(+)] and negative [eTDS(−)] scores consisted of the top 29 genes positively and 19 genes negatively associated with the TDS in the TCGA $BRAF^{V600E}$ cohort, respectively (Table 1). Also included in the eTDS were the top 10 mRNAs that positively and negatively associated with TDS over the entire TCGA cohort (all the positively correlated genes and six negatively correlated genes were also identified as part of the TCGA $BRAF^{V600E}$ cohort TDS analysis noted above). We expanded the eTDS(−) gene set to include four additional genes (SERPINA1, ELF3, EPHB3, and ATIC). The calculated MAPK output, BRAF/RAS, and TDS scores are the average fold change for all mRNAs in the gene set compared with the median of all research tissue samples. The expression changes for the eTDS gene set were scored with the following formula:

$$\text{eTDS} = \text{TDS} + \text{eTDS}(+) - \text{eTDS}(-)$$

Statistical analysis

The primary endpoint was the proportion of patients with *BRAF* mutant RAIR thyroid cancer for whom vemurafenib increased iodide incorporation to a predicted lesional absorbed dose of 2000 cGy if ≤300 mCi of ^{131}I was administered (^{124}I

Table 1. Gene Lists for BRAF-RAS, MAPK Output, TDS, and eTDS Scores

BRAF-RAS Score		MAPK Output		TDS	eTDS(+)	eTDS(−)
ABTB2	LGI3	ARID5A	KIR3DL2	DIO1	BCL2	ATIC
AHR	LLGL1	B4GALT6	LIF	DIO2	CDH16	BTG3
ANKLE2	LY6E	BRIX1	MAFF	DUOX1	CLCNKB	CBX3
ANKRD46	MDFIC	BYSL	MAP2K3	DUOX2	DLG2	ELF3
ANXA1	MET	CCND1	MYC	FOXE1	DPP6	EPHB3
ANXA2P2	MLEC	CD3EAP	NOP16	GLIS3	FAM167A	FN1
ARNTL	NQO1	CHSY1	PHLDA2	NKX2-1	FHL1	GALE
ASAP2	PDE5A	CXCL8	PLK3	PAX8	FLRT1	ITGA3
BID	PDLIM4	DDX21	POLR1C	SLC26A4	GPM6A	KCNK1
CDC42EP1	PLCD3	DUSP4	POLR3G	SLC5A5	GRIN2C	KCNN4
COL8A2	PLEKHA6	DUSP6	PPAN	SLC5A8	HGD	MAPKAPK3
CREB5	PNPLA5	EGR1	PPAT	TG	KIT	PDLIM4
CTSC	PPL	ELOVL6	PYCRL	THRA	LMOD1	PHF23
CYB561	PRICKLE1	ETV1	RRS1	THRB	LOC286002	PLP2
CYP1B1	PROS1	ETV4	SEMA6A	TPO	LRP2	PRSS22
DCSTAMP	PTPRE	ETV5	SH2B3	TSHR	MATN2	PVRL4
DTX4	PVRL4	FOS	SLC1A5		MPPED2	SERPINA1
DUSP5	RASGEF1B	FOSL1	SLC4A7		MT1G	TMEM41A
ETHE1	RUNX1	GEMIN4	SPRED2		PKHD1L1	UBE2I
EVA1A	RUNX2	GNL3	SPRY2		PLA2R1	
FAM20C	SDC4	GPR3	SPRY4		SLC26A7	
FCHO1	SEL1L3	GTF2A1L	TNC		SLC4A4	
FLJ23867	SFTPB	GTPBP4	TNFRSF12A		SORBS2	
FN1	SFTPC	HMGA2	TSR1		STXBP5L	
FSTL3	SLC35F2	HYDIN	WDR3		TFCP2L1	
GABRB2	SLC4A4	IER3	YRDC		TFF3	
GBP2	SORBS2				TPPP	
GNA14	SOX4				WSCD2	
HGD	SPOCK2				ZMAT4	
ITGA3	STK17B					
ITGB8	SYT12					
KATNAL2	TACSTD2					
KCNAB1	TBC1D2					
KCNIP3	TGFBR1					
KCNN4	TMEM43					
LAMB3						

responder). Assuming the true response rate with this approach is <5%, the probability of seeing two or more responses in 10 untreated patients is <10%. Therefore, two or more responses were considered indicative of a response rate being >5% at a 0.1 significance level. Patients who were removed from study before the second ^{124}I PET were considered unevaluable and replaced. All ^{124}I SUV_{max} values reported here were calculated with volume correction. Secondary endpoints included best overall response and progression-free survival [per Response Evaluation Criteria in Solid Tumors (RECIST) version 1.1] 6 months after ^{131}I, quantification of serial TGs, and assessment of vemurafenib safety and tolerability. The Wilcoxon rank-sum test was applied for the comparison between serum TG values in the ^{124}I responder and nonresponder groups. Toxicity with vemurafenib alone or in combination with ^{131}I was assessed as per Common Terminology Criteria for Adverse Events version 4.0 from the start of vemurafenib until 30 days after the last dose of the drug.

Results

Baseline characteristics

Between June 2014 and January 2016, 12 $BRAF^{V600E}$ mutant patients were enrolled. The clinical characteristics of all enrolled patients are included in Table 2. All patients had received at least one RAI treatment. One patient was previously treated with a TKI (sorafenib). All 12 had RAI nonavid lesions on the baseline ^{124}I PET/CT: eight lacked detectable ^{124}I in all tumors, and four had modest ^{124}I uptake in at least one tumor site (Table 3).

Efficacy

The protocol schema is depicted in Fig. 1. Two patients were removed before the second ^{124}I PET/CT and were evaluable only for safety and tolerability: one for grade 3 palmar-plantar erythrodysesthesia (patient 3) and the other for dysphagia precluding continued drug treatment (patient 5). The remaining 10 patients underwent a second ^{124}I PET/CT scan. For six (60%) patients, the second ^{124}I PET revealed new or increased RAI avidity with vemurafenib in at least one tumor (Table 3). The degree of lesional RAI incorporation achieved among these patients was heterogeneous, including seven lesions demonstrating dramatic enhancement, with SUV_{max} values >50 (Fig. 2). Four (40%; 95% CI, 12% to

Table 2. Demographic, Clinical, and Pathologic Characteristics of the 12 Enrolled Patients

Patient/Tumor Characteristic	No. (%)
Age, y	
Median	68
Range	43–72
Sex	
Male	7
Female	5
Tumor histology, no./total no. (%)	
Classic papillary	2/12 (17)
Tall-cell variant papillary	5/12 (42)
Columnar cell papillary	2/12 (17)
Poorly differentiated carcinoma	3/12 (25)
Tumor genotype, no./total no. (%)	
BRAF V600E	12/12 (100)
Prior radioiodine treatments per patient, no.	
Median	1
Range	1–3
Other treatments for thyroid cancer, no. of patients/total no. (%)	
External-beam radiation therapy	5/12 (42)
Doxorubicin (concurrently with radiation therapy)	2/12 (17)
Vascular endothelial growth factor receptor–targeted TKI	1/12 (8)

74%) patients met the lesional dosimetry threshold for ^{131}I treatment (^{124}I responders). The four ^{124}I responders were treated with ^{131}I and vemurafenib (Table 3). Tumor histologies for these patients included columnar cell PTC (1), poorly differentiated thyroid carcinoma with tall-cell features (1), and tall-cell variant PTC (2). The six ^{124}I nonresponders discontinued vemurafenib and were removed from the study.

Eight of the 10 evaluable patients underwent radiographic assessments within ~6 weeks of completing vemurafenib (for the ^{124}I responders, scans were done before ^{131}I). Vemurafenib alone resulted in tumor regression for seven patients, including all four ^{124}I responders (−3% to −60%) and three of the four nonresponders (+3% to −31%) [Fig. 3(a)]. Three of the four ^{124}I responders experienced further tumor regression after ^{131}I [Fig. 3(b)], which was associated with lower serum thyroglobulin values than baseline [Fig. 3(c)]. Six months after ^{131}I, all four patients remained free of progression, with two confirmed partial responses (PRs; −53% and −75%) and two with stable disease (SD; −10% and −5%). In comparison, three ^{124}I nonresponders who did not receive ^{131}I continued to get serial imaging off protocol, which demonstrated tumor growth after vemurafenib was discontinued.

All four ^{124}I responders were followed beyond the protocol-mandated 6 months after ^{131}I [Fig. 3(d)]. Two received additional treatment after the protocol: patient 7 (SD) underwent radiation for a pretracheal mass ~9 months after ^{131}I, and patient 2 (PR) was observed for ~18 months after ^{131}I before restarting treatment with vemurafenib (for 19+ months as of 1 November 2017). Patients 6 and 11 remained off therapy 31+ and 22+ months after ^{131}I, respectively (as of 1 November

Table 3. Summary of Study Outcomes for the 12 Enrolled Patients

Patient No.	Thyroid Pathology	Metastatic Disease Sites	Lifetime RAI (mCi) Received Before Study (No. Given)	^{124}I Avidity at Baseline	Tumor Size Change With Vem Alone	Increased RAI Avidity With Vem? (Yes/No)	Received ^{131}I? (Yes/No)	^{131}I Administered/ MTA (mCi) (% MTA Administered)	RECIST version 1.1 Response 6 mo After ^{131}I
1	PDTC (1° TCV)	L	275 (2)	None	−27%	No	No	—	—
2	CC	B, L, NL	265 (1)	None	−27%	Yes	Yes	241/309 (78%)	PR (−53%)
3	TCV	L, NL, TB	80 (1)	None	—	—	—	—	—
4	C	B, L	75 (1)	None	+3%	No	No	—	—
5	PDTC (1° TCV)	HL, L, ML	301 (2)	+HL, ML	—	—	—	—	—
6	TCV	ML, NL, TB	201 (2)	+TB	−3%	Yes	Yes	241/510 (47%)	SD (−10%)
7	PDTC (with TCF)	L, LV, HL, ML, TB	667 (3)	None	−10%	Yes	Yes	130/248 (52%)	SD (−5%)
8	CC	L, NL, TB[a]	75 (1)	+TB[a]	−31%	No[b]	No	—	—
9	C (with TCF)	HL, L, ML, NL	101 (1)	None	−19%	Yes	No	—	—
10	TCV	L, NL	163 (1)	None	—	No	No	—	—
11	TCV	HL, L, ML	200 (1)	None	−60%	Yes	Yes	401/433 (93%)	PR (−75%)
12	TCV	L, TB[a]	196 (1)	+TB,[a] L	—	Yes	No	—	—
					Totals	6/10	4/10	—	2 PR, 2 SD

"Totals" row summarizes the observed results among the 10 patients evaluable for the primary endpoint (patients 3 and 5 were removed before the second ^{124}I PET evaluation and were not evaluable).

Abbreviations: B, bone; C, classic type; CC, columnar cell; HL, hilar lymph node; L, lung; LV, liver; ML, mediastinal lymph node; NL, neck lymph node; PDTC, poorly differentiated carcinoma; TB, thyroid bed; TCF, tall-cell features; TCV, tall-cell variant; Vem, vemurafenib. Underscore denotes sites of disease discovered only on ^{124}I PET.

[a] ^{124}I avidity visualized in the thyroid bed did *not* have a structural correlate visualized on CT.

[b] Increased ^{124}I avidity was visualized in the thyroid bed, but this was not counted as increased RAI avidity given the lack of visualized structural correlate on CT.

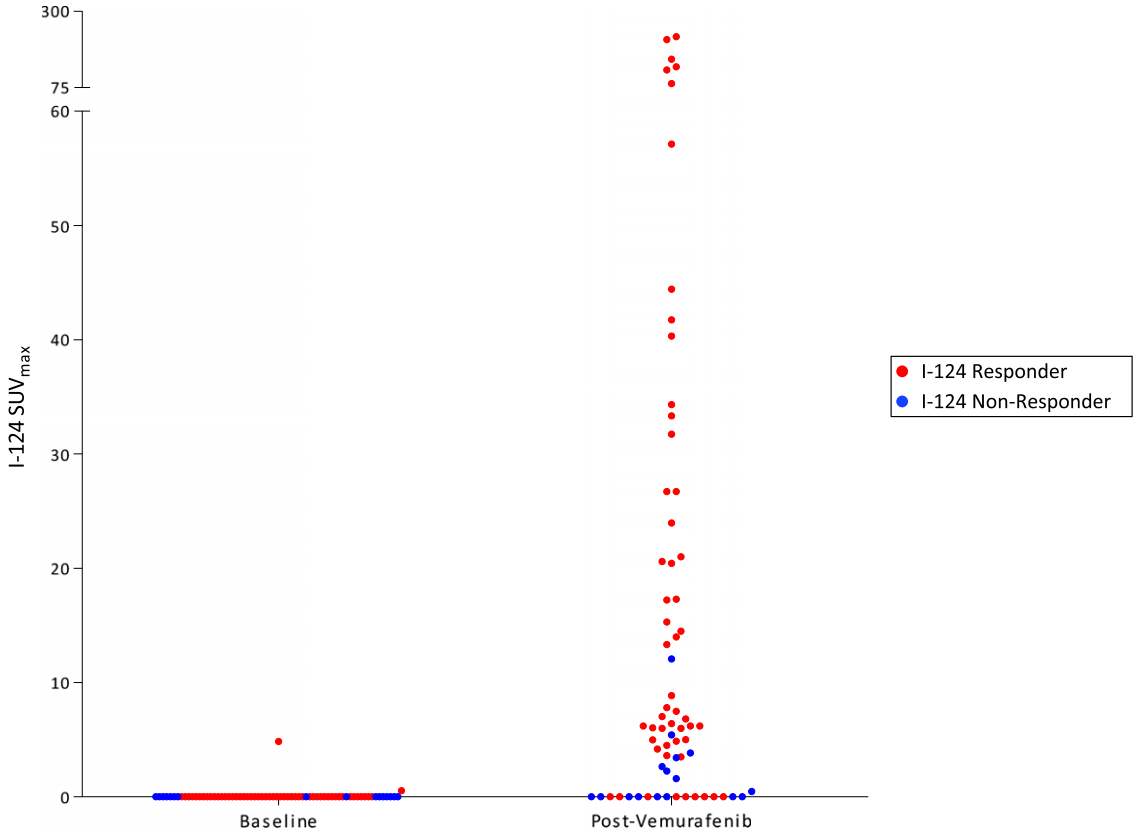

Figure 2. Lesional ^{124}I SUV_{max} values in patients with vemurafenib-mediated RAI enhancement. Baseline and on therapy ^{124}I SUV_{max} values among the six patients with vemurafenib-induced enhancement of tumor RAI avidity are shown. Each data point represents one tumor before and after vemurafenib therapy. ^{124}I responders (red) are patients 2, 6, 7, and 11; ^{124}I nonresponders (blue) are patients 9 and 12.

2017). Patient 11 has maintained an −85% regression of the RECIST right hilar lymph node target for >19 months after ^{131}I (decreased from 20 mm to 3 mm with a TSH-suppressed TG of <0.1 ng/mL, 21 months after ^{131}I). Although these parameters met criteria for complete response, this was designated clinically PR, given punctate pulmonary nodules of uncertain significance.

Safety

The most common vemurafenib toxicities observed included maculopapular rash (nine); fatigue (eight); palmar-plantar erythrodysesthesia (seven); nausea (six); arthralgia, increased bilirubin, or elevated alkaline phosphatase (five each); and alanine aminotransferase increase, diarrhea, benign neoplasm (warts), or alopecia (three each) (Table 4). Two patients had vemurafenib transiently held before completing therapy: one had a 17-day interruption for an unrelated adverse event before restarting on full dose, and the other held drug for ~4 days for grade 3 rash before restarting at 720 mg twice daily.

Analysis of clinical and molecular markers of tumor differentiation

We previously established in a *BRAF* mutant mouse model that inhibiting MAPK signaling increases RAI avidity by restoring expression of the thyroid differentiation genes responsible for iodide uptake (15, 16). To evaluate in patient tumors the biologic relationship of MAPK activity, thyroid differentiation, and RAI avidity, biopsies were performed before and during treatment (10 to 11 days on vemurafenib) in two ^{124}I responders (patients 6 and 7) and one nonresponder (patient 9). RNAseq was performed to quantify transcripts regulated by the MAPK pathway (MAPK output), the BRS (a 71-gene signature that distinguishes $BRAF^{V600E}$ tumors from *RAS* mutant tumors) (7), and the eTDS (a gene signature of thyroid-specific differentiation developed from the TCGA TDS; see Table 1 for the gene lists of each signature and the Methods section for how the eTDS was developed from the TCGA TDS) (7). The two serial biopsies were performed on the same tumor for each patient, allowing correlation of drug-induced molecular changes with ^{124}I dynamics evaluated by PET (Fig. 4). In all three patients, vemurafenib inhibited MAPK output and increased the BRS in the sampled tumors [Fig. 4(a)], consistent with a pharmacologic "reprogramming" of *BRAF* mutant expression signatures to those more similar to *RAS* mutant tumors, which have lower flux through the MAPK pathway (7). Concomitant with these signaling changes, vemurafenib increased the eTDS in all tumors [Fig. 4(a)]. The tumor from patient 6, with the highest eTDS on

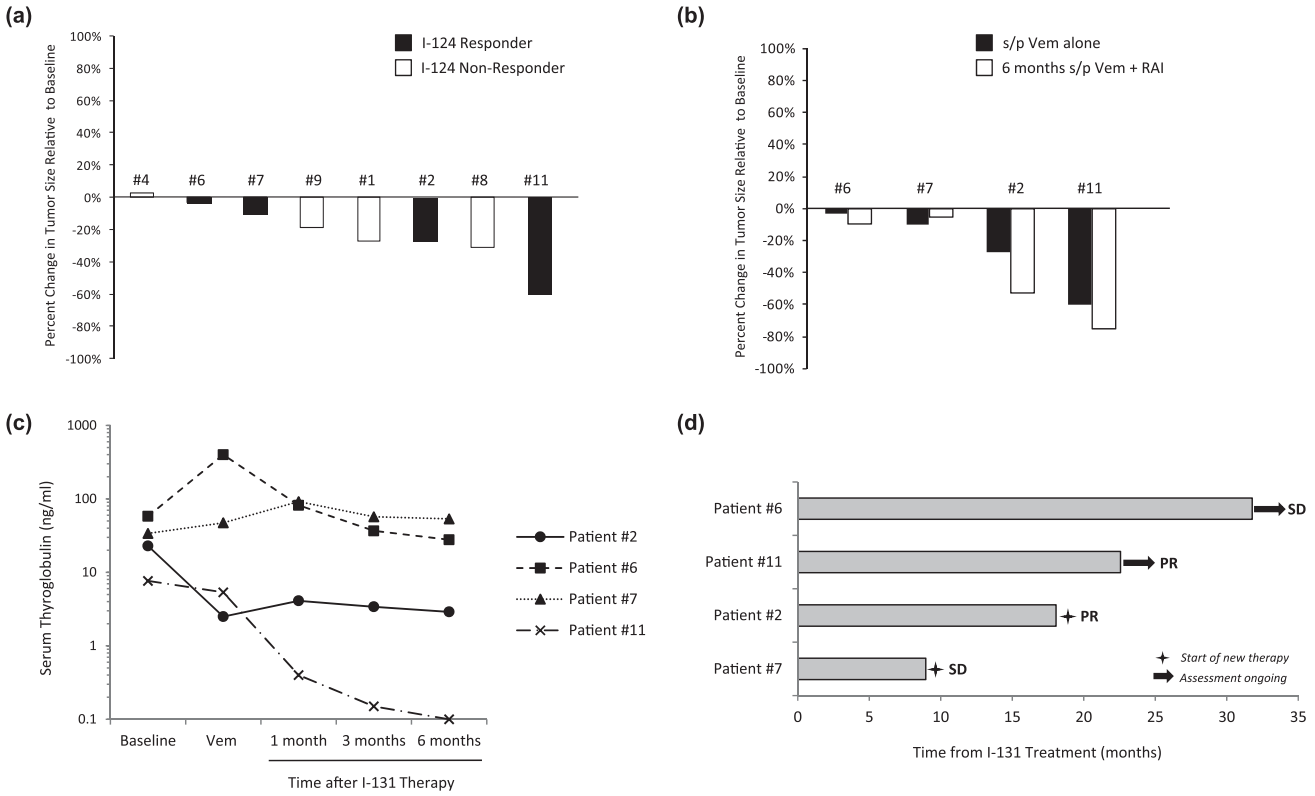

Figure 3. Efficacy of vemurafenib alone and in combination with ^{131}I. (a) Changes in tumor size after vemurafenib alone. Eight of the 10 evaluable study patients (four ^{124}I responders and four nonresponders) underwent imaging after ~4 wk of vemurafenib alone. Each bar represents the percentage change in tumor size relative to baseline observed. (b) Changes in tumor size observed among ^{124}I responders after vemurafenib alone and ~6 mo after ^{131}I, relative to baseline. (c) Serum thyroglobulin values measured in ^{124}I responders. Serum thyroglobulins were measured at baseline, after vemurafenib alone, and 1 mo, 3 mos, and 6 mo after ^{131}I. Patient 6 had detectable TG antibodies. (d) Outcomes of ^{124}I responders. Each bar represents the time each ^{124}I responder remained off therapy after vemurafenib plus ^{131}I. Two patients continued to remain off therapy as of 1 November 2017. s/p, status post; Vem, vemurafenib.

vemurafenib, also possessed the highest ^{124}I uptake (SUV_{max} of 31.7) [Fig. 4(b)], consistent with the hypothesis that the degree of RAI avidity restored is linked to the extent to which drug therapy increases the expression of the thyroid-specific genes responsible for iodine uptake and retention (16).

The TCGA analysis revealed that among *BRAF* mutant thyroid cancers there exists significant variability in the extent to which thyroid-specific gene expression is retained (7). The tumors molecularly profiled here also possessed notable differences in baseline eTDS [Fig. 4(a)], despite all initially having been RAI negative on ^{124}I PET [Fig. 4(b)]. Because TG is encoded by a thyroid differentiation gene and is a major contributor to the eTDS, we hypothesized that pretreatment serum TG could serve as a quantifiable marker of differentiation. We found that the mean pretreatment serum TG value among ^{124}I responders was significantly higher than those among nonresponders (mean: 30.6 vs 1.0 ng/mL; P = 0.0048) (Fig. 5). All nonresponders had TG values ≤2 ng/mL (range: <0.1 to 2.0 ng/mL), whereas responders had values >7 ng/mL (range: 7.7 to 58.0). This observation suggests that tumors with a higher degree of differentiation (higher serum TG) are better positioned to be successfully redifferentiated with vemurafenib therapy than less differentiated tumors at baseline.

Discussion

This study achieved the primary endpoint of demonstrating that vemurafenib increases iodide incorporation in RAIR *BRAF* mutant patients (six out of 10 with new RAI incorporation, four treated with ^{131}I). These results are superior to those observed with the MEK inhibitor selumetinib (four out of nine with increased RAI; one received ^{131}I) (17) and similar to data with the BRAF inhibitor dabrafenib (6 out of 10 patients with new or increased RAI) (27). Those treated with ^{131}I experienced clinical benefit for >6 months after therapy, including one patient with near complete regression of the target lesion and an undetectable TSH-suppressed TG ~21 months after therapy. Disease control without the need for continuous drug administration and toxicity is the advantage of this redifferentiation approach over TKIs that currently

Table 4. Vemurafenib-Related Adverse Events, All Grades

Toxicity	Grade 1	Grade 2	Grade 3	Grade 4	Grade 5	Total
Maculopapular rash	5	2	2			9
Fatigue	8					8
Palmar-plantar erythrodysesthesia syndrome	3	3	1			7
Nausea	6					6
Alkaline phosphatase increased	5					5
Arthralgia	5					5
Bilirubin increased	4	1				5
Alanine aminotransferase increased	3					3
Diarrhea	3					3
Neoplasm, benign (warts)	1	2				3
Alopecia	3					3
Skin and subcutaneous tissue disorders[a]	2					2
Creatinine increased	2					2
Aspartate aminotransferase increased	2					2
Myalgia	2					2
Dysgeusia	2					2
Pruritus	1		1			2
Anemia	1					1
Constipation	1					1
Cough	1					1
Dry skin	1					1
Hypocalcemia	1					1
Hypophosphatemia			1			1
Dehydration		1				1
Dry mouth	1					1
Eye disorders (other, specify)	1					1
Headache	1					1
Hoarseness	1					1
Mucositis oral	1					1
Oral pain	1					1
Pain	1					1
Skin hyperpigmentation	1					1
Chest wall pain	1					1

[a]Seborrheic keratosis (1 case), keratosis pilaris-like reaction (1 case).

constitute standard therapy for RAIR patients (1, 4, 28). Future trial designs will need novel study endpoints to capture the unique clinical benefits of this approach (*e.g.* proportion of patients for whom redifferentiation delays TKI initiation).

Beyond establishing that vemurafenib can increase RAI in *BRAF* mutant patients, this study investigated mechanistic questions of redifferentiation the previous selumetinib and dabrafenib trials did not address. Because response previously was assessed only after both drug and ^{131}I were administered, neither trial delineated how much of the tumor regression achieved was attributable to the short course of drug alone vs ^{131}I. This was a lesser consideration for selumetinib (17) because a separate phase II study determined that it possesses little single-agent activity in RAIR patients (29). For BRAF inhibitors, however, two trials have confirmed that vemurafenib and dabrafenib are both active agents against *BRAF* mutant RAIR disease (30, 31); vemurafenib is now a compendium-approved therapy for this indication (30). Not addressing how the direct antiproliferative activity of the drug contributed to study outcomes was raised as a confounding design element of the dabrafenib redifferentiation study (19, 32). With vemurafenib, we observed that seven of eight patients experienced tumor regression after 4 weeks of therapy, including all four of the patients who went on to receive ^{131}I. ^{131}I induced further tumor regression in three of those four patients, suggesting that the 6-month response outcomes largely represent the combined impact of vemurafenib directly on both tumor cell proliferation and redifferentiation. Importantly, three patients designated as ^{124}I nonresponders also achieved regression with the 1-month course of vemurafenib [patients 8 (−31%), 1 (−27%), and 9 (−19%)], indicating that the reprogramming of cancer cell differentiation can be uncoupled from the growth-suppressive effects of MAPK blockade.

A critical aspect of this study was the use of investigational ^{124}I PET/CT scans to quantify drug-induced changes in tumoral iodine incorporation, which predict the ^{131}I radiation dosage that can be delivered to each individual tumor (lesional dosimetry) (33, 34). This provides an advantage over the

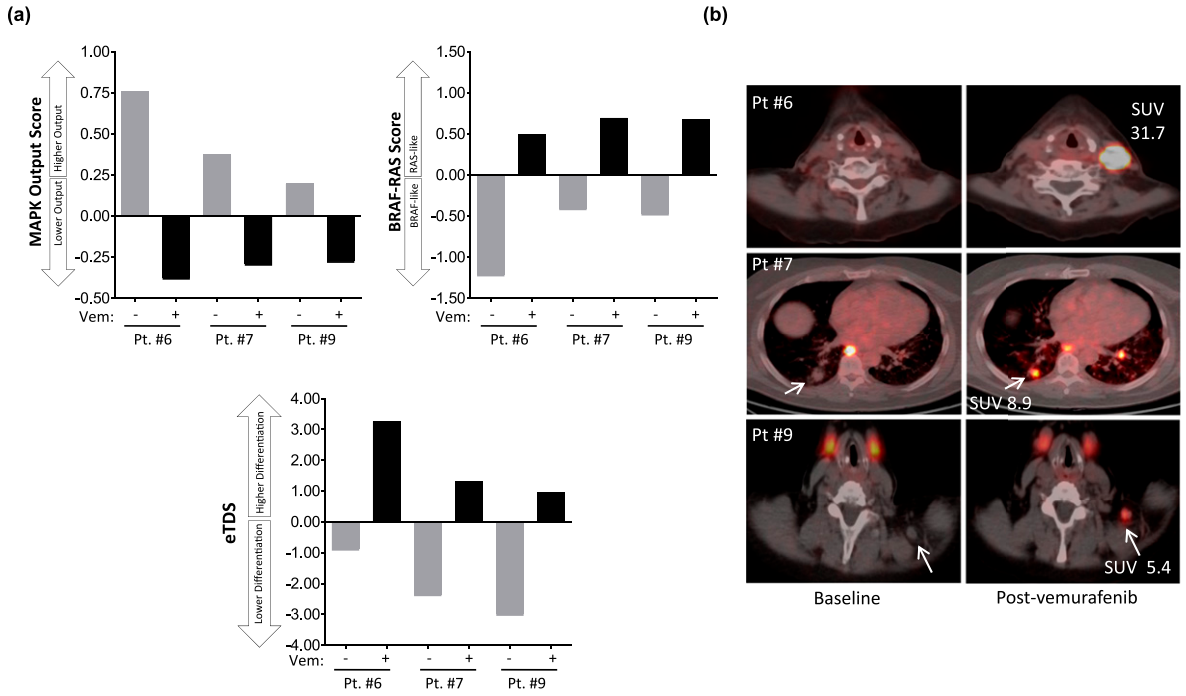

Figure 4. MAPK signaling, thyroid differentiation, and ^{124}I avidity. Two serial biopsies were performed on the same tumor for each patient, allowing correlation of drug-induced molecular changes with ^{124}I dynamics measured by PET/CT. (a) RNA was extracted from the two serial biopsies for RNAseq to quantify transcripts regulated by MAPK output, the BRS, and the eTDS. The MAPK output score, BRS, and eTDS values represent the average fold change for all mRNAs in the gene set compared with the median of all the samples. (b) Fused ^{124}I PET/CT images of the serially sampled tumors analyzed in (a). Gray bars indicate scores calculated in tumors obtained before vemurafenib. Black bars indicate scores calculated from biopsies obtained from the same tumors after 10 to 11 d on vemurafenib. Vem, vemurafenib.

traditional ^{131}I whole body scintigraphy or ^{131}I with single photon emission computed tomography/CT used in standard practice and the dabrafenib redifferentiation trial (27), methods that possess a more limited capacity for precisely quantifying RAI uptake in individual lesions. The ^{124}I lesional dosimetry approach allowed us to identify two categories of ^{124}I nonresponders: those whose tumors remained non-RAI avid on vemurafenib and those whose tumors achieved incremental RAI enhancement that was insufficient to justify treatment. Therefore, the failure to adequately redifferentiate with vemurafenib is not a singular entity and is probably modified by diverse biologic factors. Some tumors may harbor additional defects that render them irreversibly dedifferentiated, whereas others may be reprogrammable by targeting the appropriate signaling pathways. The lesion-to-lesion heterogeneity in RAI avidity within individual patients may reflect differential exposure to circulating RAI or vemurafenib, or more likely clonal biological differences between metastatic tumors. Lastly, the impact of vemurafenib on RAI uptake vs retention remains an unexplored yet important biologic question. Identifying what pathways in conjunction with MAPK activation may influence either or both of these parameters could lead to new pharmacologic approaches that could significantly increase RAI tumoral residence and efficacy.

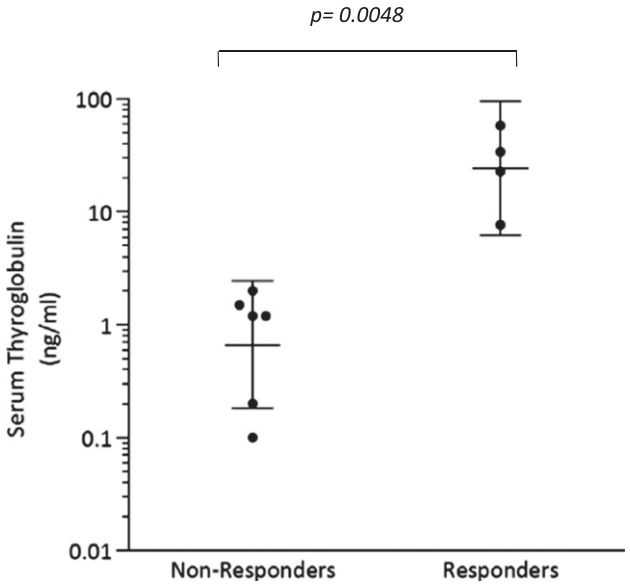

Figure 5. Baseline serum thyroglobulin values among the ^{124}I nonresponders and responders. Patient 9 (nonresponder) had a TG value of <0.1 ng/mL, which is designated here as a value of 0.1 ng/mL. Patient 6 (responder) and 9 (nonresponder) had detectable TG antibodies. Bars indicate geometric means of the values with 95% CI.

Having observed that vemurafenib may restore the efficacy of ^{131}I for a subset of patients, along with the previous phase II trial demonstrating single-agent

vemurafenib activity against RAIR disease (30), we propose that biomarkers to delineate which of these uses of vemurafenib (continuously administered vs in combination with ^{131}I) are best for an individual patient could be an important tool to personalize how BRAF inhibition is implemented. To this end, we observed that ^{124}I responders had higher baseline serum TG values compared with nonresponders. Although TG is typically used in clinical practice as a marker of tumor burden, it is also an important biomarker of thyroid differentiation (7, 15), explaining why it may predict successful RAI enhancement with vemurafenib. Importantly, these statistically significant differences in TG values were quantified in RAIR patients whose tumors were generally RAI nonavid, suggesting the possibility that distinctions in tumor differentiation can be quantified beyond what can be inferred by RAI status alone. This initial observation certainly warrants further validation in a larger data set of *BRAF* mutant patients treated with redifferentiation strategies.

However, serum TG is influenced by TSH levels and interfering TG antibodies, making it an imperfect differentiation marker in some clinical contexts. Furthermore, because iodine incorporation requires the preserved function of a complex network of genes besides TG, we propose that molecular signatures may offer a more precise and comprehensive method for quantifying thyroid differentiation that may better predict the likelihood of response to RAI. This approach first requires clinical evidence of the long-assumed hypothesis that the RAI avidity of a tumor is indeed determined by the thyroid differentiation state, that is, the degree to which it expresses the genes that mediate iodide uptake and thyroid hormone biosynthesis (*eg,* NIS, TPO, and TG). The analysis of serial research biopsies in this trial provided the clinical construct needed to examine this hypothesis as quantitative changes in MAPK signaling and thyroid differentiation gene signatures were scored and compared with the changes in ^{124}I PET uptake achieved *within the same tumor*.

As expected, we observed a direct link between the degree of molecular thyroid differentiation that was scored (eTDS) and the RAI avidity present in clinical specimens. Additionally, our data provide clinical evidence linking MAPK pathway inhibition with increased molecular differentiation (eTDS) in patients, consistent with the biologic hypothesis formulated in preclinical animal models that MAPK is a critical regulator of thyroid tumor differentiation (15, 16). However, inhibition of MAPK transcriptional output did not translate into sufficient redifferentiation in all the patients analyzed, suggesting either that more potent pathway inhibition may be needed or that biologic factors beyond MAPK inhibition may be critical. Ongoing clinical studies evaluating combinations with BRAF inhibitors to more effectively inhibit MAPK signaling should provide more insight into this question.

A clear limitation of these molecular studies is the small number of patients evaluated, primarily because of the challenge of obtaining multiple research biopsies from patients on therapy being evaluated with investigational ^{124}I PET scans. The analysis here is certainly not conclusive, but it represents important clinical proof-of-concept observations that support biologic hypotheses that to date have been developed primarily in preclinical models. Efforts to more broadly study how these molecular scores correlate to RAI efficacy will not only validate these biologic models but also serve as a molecular classification of tumor differentiation that could influence clinical decision making for the standard use of RAI and the ways redifferentiation approaches are applied in the future.

Acknowledgments

The authors acknowledge the contributions of the Memorial Sloan-Kettering Cancer Center research staff from the medical oncology and nuclear medicine services that coordinated execution of this clinical trial.

Financial Support: This investigator-initiated trial was supported by Genentech (to L.A.D.). The study was also funded in part through the National Institutes of Health (NIH)/National Cancer Institute (NCI) Cancer Center Support Grant P30 CA008748, NIH/NCI R01 CA184724 (to A.L.H.), NIH/NCI 5 R01 CA201250 (to S.M.L.), and NIH/NCI SPORE in Thyroid Cancer Grant P50 CA172012 (to J.A.F.). Support was also provided by Geoffrey Beene Cancer Research Center and Cycle for Survival at Memorial Sloan-Kettering Cancer Center (to A.L.H.). The MSK Integrated Genomics Operation Core used here for the molecular analyses was funded by the NCI Cancer Center Support Grant (CCSG, P30 CA08748), Cycle for Survival, and the Marie-Josée and Henry R. Kravis Center for Molecular Oncology.

Clinical Trial Information: ClinicalTrials.gov no. NCT02145143 (registered 22 May 2014).

Correspondence and Reprint Requests: Alan L. Ho, MD, PhD, Memorial Sloan-Kettering Cancer Center, 300 East 66th Street, New York, New York 10065. E-mail: hoa@mskcc.org.

Disclosure Summary: A.L.H has served on advisory boards or performed consulting for Genentech, Sanofi Genzyme, Eisai, AstraZeneca, Regeneron, Merck, Sun Pharmaceuticals, Ayala Pharmaceuticals, Kura Oncology, Ignyta, TRM Oncology, and Novartis. S.S.B. is currently employed by Flatiron Health (Roche). R.M.T. has performed consulting for Sanofi Genzyme and Eisai. R.A.G. has performed consulting for Veracyte. J.A.F. has received research funding from Eisai. The remaining authors have nothing to disclose.

References

1. Brose MS, Nutting CM, Jarzab B, Elisei R, Siena S, Bastholt L, de la Fouchardiere C, Pacini F, Paschke R, Shong YK, Sherman SI, Smit

JW, Chung J, Kappeler C, Peña C, Molnár I, Schlumberger MJ; DECISION investigators. Sorafenib in radioactive iodine-refractory, locally advanced or metastatic differentiated thyroid cancer: a randomised, double-blind, phase 3 trial. *Lancet*. 2014; **384**(9940):319–328.
2. Cabanillas ME, Schlumberger M, Jarzab B, Martins RG, Pacini F, Robinson B, McCaffrey JC, Shah MH, Bodenner DL, Topliss D, Andresen C, O'Brien JP, Ren M, Funahashi Y, Allison R, Elisei R, Newbold K, Licitra LF, Sherman SI, Ball DW. A phase 2 trial of lenvatinib (E7080) in advanced, progressive, radioiodine-refractory, differentiated thyroid cancer: a clinical outcomes and biomarker assessment. *Cancer*. 2015;**121**(16):2749–2756.
3. Kloos RT, Ringel MD, Knopp MV, Hall NC, King M, Stevens R, Liang J, Wakely PE, Jr, Vasko VV, Saji M, Rittenberry J, Wei L, Arbogast D, Collamore M, Wright JJ, Grever M, Shah MH. Phase II trial of sorafenib in metastatic thyroid cancer. *J Clin Oncol*. 2009;**27**(10):1675–1684.
4. Schlumberger M, Tahara M, Wirth LJ, Robinson B, Brose MS, Elisei R, Habra MA, Newbold K, Shah MH, Hoff AO, Gianoukakis AG, Kiyota N, Taylor MH, Kim SB, Krzyzanowska MK, Dutcus CE, de las Heras B, Zhu J, Sherman SI. Lenvatinib versus placebo in radioiodine-refractory thyroid cancer. *N Engl J Med*. 2015;**372**(7):621–630.
5. Blevins DP, Dadu R, Hu M, Baik C, Balachandran D, Ross W, Gunn B, Cabanillas ME. Aerodigestive fistula formation as a rare side effect of antiangiogenic tyrosine kinase inhibitor therapy for thyroid cancer. *Thyroid*. 2014;**24**:918–922.
6. Kimura ET, Nikiforova MN, Zhu Z, Knauf JA, Nikiforov YE, Fagin JA. High prevalence of BRAF mutations in thyroid cancer: genetic evidence for constitutive activation of the RET/PTC-RAS-BRAF signaling pathway in papillary thyroid carcinoma. *Cancer Res*. 2003;**63**(7):1454–1457.
7. Cancer Genome Atlas Research Network. Integrated genomic characterization of papillary thyroid carcinoma. *Cell*. 2014;**159**(3): 676–690.
8. Durante C, Puxeddu E, Ferretti E, Morisi R, Moretti S, Bruno R, Barbi F, Avenia N, Scipioni A, Verrienti A, Tosi E, Cavaliere A, Gulino A, Filetti S, Russo D. BRAF mutations in papillary thyroid carcinomas inhibit genes involved in iodine metabolism. *J Clin Endocrinol Metab*. 2007;**92**(7):2840–2843.
9. Elisei R, Ugolini C, Viola D, Lupi C, Biagini A, Giannini R, Romei C, Miccoli P, Pinchera A, Basolo F. BRAF(V600E) mutation and outcome of patients with papillary thyroid carcinoma: a 15-year median follow-up study. *J Clin Endocrinol Metab*. 2008;**93**(10): 3943–3949.
10. Knauf JA, Kuroda H, Basu S, Fagin JA. RET/PTC-induced dedifferentiation of thyroid cells is mediated through Y1062 signaling through SHC-RAS-MAP kinase. *Oncogene*. 2003;**22**(28):4406–4412.
11. Lee JH, Lee ES, Kim YS. Clinicopathologic significance of BRAF V600E mutation in papillary carcinomas of the thyroid: a meta-analysis. *Cancer*. 2007;**110**(1):38–46.
12. Liu D, Hu S, Hou P, Jiang D, Condouris S, Xing M. Suppression of BRAF/MEK/MAP kinase pathway restores expression of iodide-metabolizing genes in thyroid cells expressing the V600E BRAF mutant. *Clin Cancer Res*. 2007;**13**:1341–1349.
13. Mitsutake N, Knauf JA, Mitsutake S, Mesa C, Jr, Zhang L, Fagin JA. Conditional BRAFV600E expression induces DNA synthesis, apoptosis, dedifferentiation, and chromosomal instability in thyroid PCCL3 cells. *Cancer Res*. 2005;**65**(6):2465–2473.
14. Riesco-Eizaguirre G, Gutiérrez-Martínez P, García-Cabezas MA, Nistal M, Santisteban P. The oncogene BRAF V600E is associated with a high risk of recurrence and less differentiated papillary thyroid carcinoma due to the impairment of Na+/I− targeting to the membrane. *Endocr Relat Cancer*. 2006;**13**(1):257–269.
15. Chakravarty D, Santos E, Ryder M, Knauf JA, Liao XH, West BL, Bollag G, Kolesnick R, Thin TH, Rosen N, Zanzonico P, Larson SM, Refetoff S, Ghossein R, Fagin JA. Small-molecule MAPK inhibitors restore radioiodine incorporation in mouse thyroid cancers with conditional BRAF activation. *J Clin Invest*. 2011; **121**(12):4700–4711.
16. Nagarajah J, Le M, Knauf JA, Ferrandino G, Montero-Conde C, Pillarsetty N, Bolaender A, Irwin C, Krishnamoorthy GP, Saqcena M, Larson SM, Ho AL, Seshan V, Ishii N, Carrasco N, Rosen N, Weber WA, Fagin JA. Sustained ERK inhibition maximizes responses of BrafV600E thyroid cancers to radioiodine. *J Clin Invest*. 2016;**126**(11):4119–4124.
17. Ho AL, Grewal RK, Leboeuf R, Sherman EJ, Pfister DG, Deandreis D, Pentlow KS, Zanzonico PB, Haque S, Gavane S, Ghossein RA, Ricarte-Filho JC, Domínguez JM, Shen R, Tuttle RM, Larson SM, Fagin JA. Selumetinib-enhanced radioiodine uptake in advanced thyroid cancer. *N Engl J Med*. 2013;**368**(7):623–632.
18. Poulikakos PI, Zhang C, Bollag G, Shokat KM, Rosen N. RAF inhibitors transactivate RAF dimers and ERK signalling in cells with wild-type BRAF. *Nature*. 2010;**464**(7287):427–430.
19. Rothenberg SM, Daniels GH, Wirth LJ. Redifferentiation of iodine-refractory BRAF V600E-mutant metastatic papillary thyroid cancer with dabrafenib—response. *Clin Cancer Res*. 2015;**21**: 5640–5641.
20. Wang W, Larson SM, Tuttle RM, Kalaigian H, Kolbert K, Sonenberg M, Robbins RJ. Resistance of [18f]-fluorodeoxyglucose-avid metastatic thyroid cancer lesions to treatment with high-dose radioactive iodine. *Thyroid*. 2001;**11**:1169–1175.
21. Van Nostrand D, Moreau S, Bandaru VV, Atkins F, Chennupati S, Mete M, Burman K, Wartofsky L. (124)I positron emission tomography versus (131)I planar imaging in the identification of residual thyroid tissue and/or metastasis in patients who have well-differentiated thyroid cancer. *Thyroid*. 2010;**20**:879–883.
22. Benua RS, Cicale NR, Sonenberg M, Rawson RW. The relation of radioiodine dosimetry to results and complications in the treatment of metastatic thyroid cancer. *Am J Roentgenol Radium Ther Nucl Med*. 1962;**87**:171–182.
23. Robbins RJ, Larson SM, Sinha N, Shaha A, Divgi C, Pentlow KS, Ghossein R, Tuttle RM. A retrospective review of the effectiveness of recombinant human TSH as a preparation for radioiodine thyroid remnant ablation. *J Nucl Med*. 2002;**43**(11):1482–1488.
24. Van Nostrand D, Atkins F, Moreau S, Aiken M, Kulkarni K, Wu JS, Burman KD, Wartofsky L. Utility of the radioiodine whole-body retention at 48 hours for modifying empiric activity of 131-iodine for the treatment of metastatic well-differentiated thyroid carcinoma. *Thyroid*. 2009;**19**:1093–1098.
25. Tala H, Robbins R, Fagin JA, Larson SM, Tuttle RM. Five-year survival is similar in thyroid cancer patients with distant metastases prepared for radioactive iodine therapy with either thyroid hormone withdrawal or recombinant human TSH. *J Clin Endocrinol Metab*. 2011;**96**(7):2105–2111.
26. Pratilas CA, Taylor BS, Ye Q, Viale A, Sander C, Solit DB, Rosen N. (V600E)BRAF is associated with disabled feedback inhibition of RAF-MEK signaling and elevated transcriptional output of the pathway. *Proc Natl Acad Sci USA*. 2009;**106**(11):4519–4524.
27. Rothenberg SM, McFadden DG, Palmer EL, Daniels GH, Wirth LJ. Redifferentiation of iodine-refractory BRAF V600E-mutant metastatic papillary thyroid cancer with dabrafenib. *Clin Cancer Res*. 2015;**21**:1028–1035.
28. Cabanillas ME, de Souza JA, Geyer S, Wirth LJ, Menefee ME, Liu SV, Shah K, Wright J, Shah MH. Cabozantinib as salvage therapy for patients with tyrosine kinase inhibitor-refractory differentiated thyroid cancer: results of a multicenter phase II International Thyroid Oncology Group trial. *J Clin Oncol*. 2017;**35**(29): 3315–3321.
29. Hayes DN, Lucas AS, Tanvetyanon T, Krzyzanowska MK, Chung CH, Murphy BA, Gilbert J, Mehra R, Moore DT, Sheikh A, Hoskins J, Hayward MC, Zhao N, O'Connor W, Weck KE, Cohen RB, Cohen EE. Phase II efficacy and pharmacogenomic study of selumetinib (AZD6244; ARRY-142886) in iodine-131 refractory papillary thyroid carcinoma with or without follicular elements. *Clin Cancer Res*. 2012;**18**:2056–2065.

30. Brose MS, Cabanillas ME, Cohen EE, Wirth LJ, Riehl T, Yue H, Sherman SI, Sherman EJ. Vemurafenib in patients with BRAF (V600E)-positive metastatic or unresectable papillary thyroid cancer refractory to radioactive iodine: a non-randomised, multicentre, open-label, phase 2 trial. *Lancet Oncol*. 2016;**17**(9): 1272–1282.
31. Shah MH, Wei L, Wirth LJ, Daniels GH, De Souza JA, Timmers CD, Sexton JL, Beshara M, Nichols D, Snyder N, Devine CE, Konda B, Busaidy NL. Results of randomized phase II trial of dabrafenib versus dabrafenib plus trametinib in BRAF-mutated papillary thyroid carcinoma. *Journal of Clinical Oncology* 2017; **35**(15 suppl):6022.
32. Huillard O, Tenenbaum F, Clerc J, Goldwasser F, Groussin L. Redifferentiation of iodine-refractory BRAF V600E-mutant metastatic papillary thyroid cancer with dabrafenib—letter. *Clin Cancer Res*. 2015;**21**:5639.
33. Pentlow KS, Graham MC, Lambrecht RM, Daghighian F, Bacharach SL, Bendriem B, Finn RD, Jordan K, Kalaigian H, Karp JS, Robeson WR, Larson SM. Quantitative imaging of iodine-124 with PET. *J Nucl Med*. 1996;**37**(9):1557–1562.
34. Sgouros G, Kolbert KS, Sheikh A, Pentlow KS, Mun EF, Barth A, Robbins RJ, Larson SM. Patient-specific dosimetry for ^{131}I thyroid cancer therapy using ^{124}I PET and 3-dimensional-internal dosimetry (3D-ID) software. *J Nucl Med*. 2004;**45**(8):1366–1372.